Eur. Phys. J. D **41**, 211–219 (2007)
DOI: 10.1140/epjd/e2006-00229-5

THE EUROPEAN PHYSICAL JOURNAL D

Decay of metastable states in Nd II

É. Biémont[1,2,a], A. Ellmann[3], P. Lundin[3], S. Mannervik[3], L.-O. Norlin[4], P. Palmeri[1], P. Quinet[1,2], D. Rostohar[2,3], P. Royen[3], and P. Schef[3]

[1] Astrophysique et Spectroscopie, Université de Mons-Hainaut, Rue de la Halle 15, 7000 Mons, Belgium
[2] IPNAS (Bât. B15), Université de Liège, 4000 Liège, Belgium
[3] Physics Department, Stockholm University, AlbaNova University Center, 10691 Stockholm, Sweden
[4] Physics Department, Royal Institute of Technology, AlbaNova University Center, 10691 Stockholm, Sweden

Received 18 February 2006 / Received in final form 20 September 2006
Published online 13 October 2006 –

Abstract. The difficulty associated with an accurate determination of transition rates for forbidden lines in lowly ionized heavy elements is illustrated in the case of Nd II. We have investigated the radiative decay of the low-lying metastable levels in Nd^+ including the two levels $4f^4(^5I)5d\ ^6K_{11/2}$ and $4f^4(^5I)5d\ ^6I_{13/2}$. In these two particular cases, using different theoretical approaches, we find that the decay is dominated by the M1 channels but that the E2 contributions are of the same order of magnitude. These levels have also been studied experimentally by lifetime measurements with the heavy ion storage ring CRYRING of Stockholm University. The difficulties encountered when performing such experiments are underlined and discussed.

PACS. 31.25.-v Electron correlation calculations for atoms and molecules – 39.10.+j Atomic and molecular beam sources and techniques

1 Introduction

Neodymium ($Z = 60$) is present in the solar system in the form of seven stable and nine short-lived isotopes and isomers. In stellar nucleosynthesis, ^{142}Nd (27%) is a pure s process product, ^{143}Nd (12%), ^{144}Nd (24%), ^{145}Nd (8%) and ^{146}Nd (17%) are produced by either the r or the s process and ^{148}Nd (6%) and ^{150}Nd (6%) are both generated by pure r process. In astrophysics, Nd^+ transitions have been identified in many types of stars including e.g. the Ap stars of the Cr-Eu-Sr subgroup [1], Bp stars of the Si subgroup [2], Am stars [3], Ba stars where large overabundances of this element are observed [4] and the sun [5,6]. Besides the interest of investigating Nd lines in relation with the determination of the chemical composition of the astrophysical objects, Nd is also important in cosmochronology because it can be used as a nuclear chronometer [7].

The metastable states play a particular role in this context because they correspond to low energy levels which are generally easily populated in stellar atmospheres and because they are able to emit strong lines in low-density media where they appear as diagnostic tools for temperature and density determinations in the plasmas.

The investigation of the radiative properties of the heavy elements, particularly those of lanthanide group, is a very complex task both theoretically and experimentally. The recent recording, with the Hubble Space Telescope, of a large number of astrophysical spectra, characterized by a high resolution and a high signal-to-noise ratio, has put forward the need of a huge amount of accurate atomic data for their interpretation (see e.g. [8]). Theoretically, the difficulty to calculate accurately the atomic structures of these heavy elements is related to the necessity to consider simultaneously, in the models, relativity and correlation effects, most of the spectra of the group being strongly perturbed. An additional difficulty results from the structural complexity associated with the progressive filling, from La to Lu, of the $4f$ shell. As a result, the calculated lifetimes (or transition probabilities) are depending, in a very sensitive way, upon the mixing occurring among the different configurations.

In the present paper, 3 different independent theoretical approaches are used for calculating lifetimes of low-lying metastable states in the $4f^46s$ and $4f^45d$ even configurations of Nd II. These methods have been successful, in a recent past, for predicting radiative quantities for many rare-earth (RE) ions (see e.g. the references quoted in [9,10] and the database DREAM [11]).

We have also performed extensive experimental investigations by the Laser Probing Technique (LPT) in the ion storage ring CRYRING at Stockholm University. This method has successfully been utilized for a large number of metastable levels in different elements (see e.g the

[a] e-mail: e.biemont@ulg.ac.be

review article [12]). In this context it can be noted that the method has been used to determine lifetimes of metastable levels in two other rare earth elements, La II [13] and Eu II [14]. The studies of Nd^+, however, turned out to be very difficult and it was hard to maintain stable conditions long enough to enable accurate determination of the lifetimes.

2 Previous work

The identified configurations in Nd^+ are $4f^46s$, $4f^45d$ and $4f^35d6p$ for the even parity and $4f^35d^2$, $4f^35d6s$ and $4f^46p$ for the odd parity [15]. A revised interpretation of the spectrum of Nd II is due to Blaise et al. [16]. Below 8010 cm^{-1} [16], the even levels can decay only through M1 and E2 channels while, above that limit, in some cases, E1 contributions corresponding to infrared $4f^45d - 4f^35d^2$ transitions can eventually contribute to the decays. In such cases, the determination of the lifetimes of the metastable states requires the evaluation of the contributions arising from both the allowed and the forbidden transitions.

In Nd II, the radiative parameters are still rather poorly known even for the allowed transitions. Among the early contributions to the E1 transition rates, we must mention the arc measurements of Corliss and Bozman [17] and the branching fraction (BF) measurements of Maier and Whaling [5] who were able to deduce oscillator strengths from previous lifetime measurements [18].

Solar investigations of neodymium motivated additional measurements by Ward et al. [19,20] who used the laser-ion beam technique, and deduced oscillator strengths of some E1 Nd II lines from a combination of the BFs deduced from arc spectra [17,21] or measured by Maier and Whaling [5].

The lifetime compilation of Blagoev and Komarovskii [22] contains 11 lifetime values originating from delayed-coincidence measurements [23]. Additional measurements of radiative lifetimes in Nd II have been carried out by Pinciuc et al. [24] (35 levels) using the collinear beam-laser method, by Lu et al. [25] and Shi et al. [26] who concentrated on the odd level at 23537 cm^{-1} ($J = 9/2$) using the time-resolved collinear fast-beam laser approach. Recent measurements in the same ion were undertaken by Scholl et al. [27] using two variants of the beam-laser method and by Xu et al. [28] who used a time-resolved laser-induced fluorescence technique for 24 levels of Nd II in the energy range 20500–32500 cm^{-1}.

To the best of our knowledge, there are no published lifetime values for metastable states of Nd II and no theoretical or experimental transition probabilities are available so far for forbidden lines (M1 or E2 transitions) in this ion.

3 Calculations

The choice of a theoretical method for calculating transition probabilities in the lanthanides is complicated, in the case of ab initio approaches, by the strong collapse of the $4f$ orbital occurring in lanthanum and observed along the whole group (see e.g. [9]) and by the huge number of levels arising from the configurations involving an open $4f$ shell. Configuration interaction (CI) and relativistic effects, which are expected to be important in such heavy atoms or ions, must be considered simultaneously in the calculations.

Basically, this choice relies on partly relativistic methods based on the Schrödinger equation (like the HFR method [29]) or on fully relativistic techniques like the multiconfigurational Dirac-Fock or MCDF method) which are expected to be a priori adequate. The MCDF method should be more accurate than the HFR one for heavy ions but is more computer time consuming. Fewer convergence problems, however, do occur when using the HFR approach than the MCDF one.

In the present work, three independent theoretical methods were considered for the calculations and, from their comparisons, it was possible to assess their reliability (see hereafter). M1 and E2 transition rates were estimated for lines depopulating the first 29 Nd II metastable even-parity levels situated between 513.322 ($J = 9/2$) and 10337.097 ($J = 13/2$) cm^{-1}.

The pseudo-relativistic Hartree-Fock (HFR) method was the first approach considered [29] with two different physical models. In the first one [HFR(A)], only the $4f^45d$ and $4f^46s$ configurations were explicitly included in the calculations and the radial parameters were optimized using a well-established least-squares fitting procedure of the Hamiltonian eigenvalues to the experimental level energies [15,16]. The fitted parameters, not reproduced here, are available upon request to the authors. In the second one [HFR(B)], the set of interacting configurations was considerably extended by including single and double excitations from the $4f^45d$ and $4f^46s$ configurations of interest, i.e. by considering also $4f^35d6p$, $4f^36s6p$, $4f^25d^26s$, $4f^25d6s^2$ and $4f^25d^3$. No fitting procedure was attempted in the HFR(B) calculation.

In the second approach, the purely relativistic multiconfigurational Dirac-Fock (MCDF) method was used with the GRASP92 code as developed by Parpia et al. [30].

Eight GRASP92 calculations have been carried out. In the first one, the 1160 interacting relativistic configuration state functions (CSF) belonging to the $4f^45d$ and $4f^46s$ non relativistic configurations were considered in the framework of the Extended Average Level (EAL) option. It helped us in isolating the main decay branches of the first 29 low-lying even metastable levels. The others consisted in considering the interactions amongst the following non-relativistic configurations: $4f^45d$, $4f^46s$, $4f^47s$, $4f^46d$, $4f^35d6p$, $4f^36s6p$, $4f^35d5f$, $4f^36s5f$, $4f^36p6d$, $4f^36p7s$, $4f^25d^26s$, $4f^25d5f^2$, $4f^26s5f^2$, $4f^25d6s^2$ and $4f^25d^3$. In order to maintain the Hamiltonian matrix size tractable to our computer, we limited each calculation to only 3 symmetries (pairs of total angular momentum, J, and parity, π). Each calculation was performed in 3 steps. The first step was common to all the calculations and consisted in considering the 32 CSF with $J = 7/2$ belonging

to the ground configuration $4f^4 6s$ and optimizing the core orbitals ($1s - 5p$) along with the $4f$ and $6s$ orbitals minimizing the ground level within the framework of the Optimal Level (OL) option.

In what follows, specific details concerning the second and third steps of each calculation are given. For the purpose of getting the lifetimes of the levels at 513.322 cm^{-1} ($J = 9/2$), 1470.097 cm^{-1} ($J = 11/2$), 1650.199 cm^{-1} ($J = 9/2$), 3066.750 cm^{-1} ($J = 11/2$), 4437.558 cm^{-1} ($J = 11/2$), 6005.271 cm^{-1} ($J = 9/2$), 6931.800 cm^{-1} ($J = 11/2$), 7524.740 cm^{-1} ($J = 7/2$), 8420.321 cm^{-1} ($J = 9/2$), 9198.395 cm^{-1} ($J = 7/2$) and 9357.906 cm^{-1} ($J = 11/2$), the second step of the second calculation consisted in including the interactions amongst the configurations with $J = 7/2, 9/2, 11/2$ with occupied $4f$, $6s$, $6p$ and $5d$ orbitals. The latters were optimized minimizing an energy functional built with the 10 lowest eigenvalues using the Extended Optimal Level (EOL) option. All the other orbitals were kept frozen to the values of the first step. The number of CSF was 2651. In the third step, the configuration interaction (CI) expansion was extended to the remaining configurations listed above keeping the constraint on the value of J. This generated 10362 CSF. The $6d$, $7s$ and $5f$ orbitals were optimized, keeping all the others frozen to the values of the preceding step, by minimizing the 15 lowest eigenvalues within the framework of the EOL option. A third calculation was focused on the lifetimes of the levels at 2585.453 cm^{-1} ($J = 13/2$), 5487.657 cm^{-1} ($J = 13/2$) and 7950.070 cm^{-1} ($J = 13/2$). The second and the third steps were similar to the ones of the second calculation except that $J = 9/2, 11/2, 13/2$ and, consequently, the numbers of CSF were 2283 in the second step and 9314 in the third step. In the fourth calculation, the lifetimes of the levels at 3801.917 cm^{-1} ($J = 15/2$), at 6637.411 cm^{-1} ($J = 15/2$) and at 9042.743 cm^{-1} ($J = 15/2$) were considered. Here again both steps were similar to the ones of the second calculation with the following differences: $J = 11/2, 13/2, 15/2$; the numbers of CSF were 1770 and 7645 in the second and the third steps, respectively; the energy functionals were built with the 15 lowest eigenvalues in both steps. In order to obtain the lifetimes of the levels at 5085.619 cm^{-1} ($J = 17/2$), 5985.571 cm^{-1} ($J = 15/2$), 7868.896 cm^{-1} ($J = 17/2$) and 10194.786 cm^{-1} ($J = 17/2$), both steps of the fifth calculation were carried out similarly to the second calculation except that here $J = 13/2, 15/2, 17/2$; the numbers of CSF were 1241 in the second step and 5761 in the third step, and the energy functionals were built with the 15 lowest eigenvalues in both steps. The sixth calculation was dedicated to the lifetimes of the level at 9166.209 cm^{-1} ($J = 19/2$). Both steps were again similar to the ones of the second calculation but with $J = 15/2, 17/2, 19/2$; the numbers of CSF were 772 and 3963 in the second and the third steps, respectively; in both steps, the energy functional was built with the 10 lowest eigenvalues. In the seventh calculation, the lifetime of the level at 8796.378 cm^{-1} ($J = 5/2$) was considered. Both steps were similar again to the ones of the second calculation but with $J = 5/2, 7/2, 9/2$; the numbers of CSF were 2768 and 10464 in the second and the third steps, respectively, and the energy functionals were constructed from the 10 lowest eigenvalues in both steps. Finally, the eighth calculation was focused on the lifetime of the level at 8716.462 cm^{-1} ($J = 3/2$). In this case, $J = 3/2, 5/2, 7/2$ and the numbers of CSF were 2538 and 9375 in the second and the third steps, respectively; in both steps, the energy functional was built with the 5 lowest eigenvalues.

The levels at 9674.844 cm^{-1} ($J = 5/2$), 9877.173 cm^{-1} ($J = 9/2$), 9908.650 cm^{-1} ($J = 7/2$), and 10337.097 cm^{-1} ($J = 13/2$) have their main decay branches involving more than 3 symmetries and therefore the A-values and lifetimes were derived from the first calculation.

All the calculations were performed in both gauges (Babushkin and Coulomb) for each E2 transition. Even with several thousands of CSF, the agreement between the two gauges was still unsatisfying for some weak transitions (differences reaching sometimes a factor of 2 or more). This is not surprising for such a complex atomic structure. In Table 1, the GRASP92 A-values and lifetimes are given in the Babushkin gauge for comparison with both HFR calculations that were carried out in the length gauge.

The third theoretical method used was the one implemented in the AUTOSTRUCTURE (AST) program, an extension by Badnell [31,32] of the code SUPERSTRUCTURE [33], which computes the atomic structure within a statistical Thomas-Fermi-Dirac potential $V(\lambda_{nl})$ [34] where the λ_{nl} scaling parameters are optimized variationally by minimizing a weighted sum of the LS term energies. Unfortunately, in that case, when including both $4f^4 5d$ and $4f^4 6s$, we were unable to reproduce in a satisfying way the energy difference between these two configurations even when trying different variational optimization approaches. Indeed, when considering both configurations together, it was found that all energy levels within the $4f^4 5d$ configuration were situated about 10000 cm^{-1} too high. This shift was clearly too large to be reduced by using semi-empirical corrections. It was also verified that the inclusion of additional configurations with 3 or 2 electrons in the 4f subshell did not improve upon the situation. Consequently, only the $4f^4 5d$ configuration was included in the model in order to be able to compute at least the M1 contributions within this configuration. Semi-empirical term energy corrections (TEC) were considered in order to reduce as much as possible the discrepancies between theoretical and experimental energy levels.

Calculated transition probabilities (A_{ki}, in s^{-1}) and radiative lifetimes, as obtained with the HFR and GRASP92 calculations, are listed in Table 1. When looking at this table, we can observe a good agreement between the results obtained using the two different theoretical approaches. It is interesting to note that HFR(A) and HFR(B) results are very close indicating that the explicit consideration of additional even parities has a marginal effect on the lifetime values. Large discrepancies between HFR and GRASP results are only observed for the level at 1650 cm^{-1}.

Table 1. Calculated lifetimes for low-lying even metastable levels in Nd II and the corresponding decay rates.

Upper level		Lower level		Type	$A_{ki}(\mathrm{s}^{-1})$		
Energy[a] (cm^{-1})	Designation	Energy[a] (cm^{-1})	Designation		HFR(A)[b]	HFR(B)[c]	GRASP[d]
513.322	$4f^4(^5\mathrm{I})6s\ ^6\mathrm{I}_{9/2}$	0.000	$4f^4(^5\mathrm{I})6s\ ^6\mathrm{I}_{7/2}$	M1	0.0082	0.0086	0.0095
				$\tau =$	**121.4 s**	**116.1s**	**105.4 s**
1470.097	$4f^4(^5\mathrm{I})6s\ ^6\mathrm{I}_{11/2}$	513.322	$4f^4(^5\mathrm{I})6s\ ^6\mathrm{I}_{9/2}$	M1	0.0797	0.0817	0.0858
				$\tau =$	**12.6 s**	**12.2 s**	**11.7 s**
1650.199	$4f^4(^5\mathrm{I})6s\ ^4\mathrm{I}_{9/2}$	0.000	$4f^4(^5\mathrm{I})6s\ ^6\mathrm{I}_{7/2}$	M1	0.1010	0.0866	0.0588
		513.322	$4f^4(^5\mathrm{I})6s\ ^6\mathrm{I}_{9/2}$	M1	0.0019	0.0017	0.0013
				$\tau =$	**9.7 s**	**11.3 s**	**16.6 s**
2585.453	$4f^4(^5\mathrm{I})6s\ ^6\mathrm{I}_{13/2}$	1470.097	$4f^4(^5\mathrm{I})6s\ ^6\mathrm{I}_{11/2}$	M1	0.1321	0.1336	0.1369
				$\tau =$	**7.6 s**	**7.5 s**	**7.3 s**
3066.750	$4f^4(^5\mathrm{I})6s\ ^4\mathrm{I}_{11/2}$	513.322	$4f^4(^5\mathrm{I})6s\ ^6\mathrm{I}_{9/2}$	M1	0.0097	0.0105	0.0145
		1470.097	$4f^4(^5\mathrm{I})6s\ ^6\mathrm{I}_{11/2}$	M1	0.0027	0.0024	0.0019
		1650.199	$4f^4(^5\mathrm{I})6s\ ^4\mathrm{I}_{9/2}$	M1	0.1542	0.1492	0.1414
				$\tau =$	**6.0 s**	**6.1 s**	**6.3 s**
3801.917	$4f^4(^5\mathrm{I})6s\ ^6\mathrm{I}_{15/2}$	2585.453	$4f^4(^5\mathrm{I})6s\ ^6\mathrm{I}_{13/2}$	M1	0.1400	0.1406	0.1427
				$\tau =$	**7.1 s**	**7.1 s**	**7.0 s**
4437.558	$4f^4(^5\mathrm{I})5d\ ^6\mathrm{L}_{11/2}$	0.000	$4f^4(^5\mathrm{I})6s\ ^6\mathrm{I}_{7/2}$	E2	0.0063	0.0062	0.0054
		513.322	$4f^4(^5\mathrm{I})6s\ ^6I_{9/2}$	E2	0.0003	0.0004	0.0003
				$\tau =$	**150.7 s**	**152.1 s**	**175.6 s**
4512.481	$4f^4(^5\mathrm{I})6s\ ^4\mathrm{I}_{13/2}$	1470.097	$4f^4(^5\mathrm{I})6s\ ^6\mathrm{I}_{11/2}$	M1	0.0026	0.0027	0.0046
		2585.453	$4f^4(^5\mathrm{I})6s\ ^6\mathrm{I}_{13/2}$	M1	0.0023	0.0020	0.0028
		3066.750	$4f^4(^5\mathrm{I})6s\ ^4\mathrm{I}_{11/2}$	M1	0.1650	0.1629	0.1570
				$\tau =$	**5.8 s**	**5.9 s**	**6.1 s**
5085.619	$4f^4(^5\mathrm{I})6s\ ^6\mathrm{I}_{17/2}$	3801.917	$4f^4(^5\mathrm{I})6s\ ^6\mathrm{I}_{15/2}$	M1	0.0944	0.0950	0.0960
				$\tau =$	**10.6 s**	**10.5 s**	**10.4 s**
5487.657	$4f^4(^5\mathrm{I})5d\ ^6\mathrm{L}_{13/2}$	513.322	$4f^4(^5\mathrm{I})6s\ ^6\mathrm{I}_{9/2}$	E2	0.0080	0.0081	0.0080
		4437.558	$4f^4(^5\mathrm{I})5d\ ^6\mathrm{L}_{11/2}$	M1	0.0921	0.0914	0.0918
				$\tau =$	**9.9 s**	**9.9 s**	**10.0 s**
5985.571	$4f^4(^5\mathrm{I})6s\ ^4\mathrm{I}_{15/2}$	3801.917	$4f^4(^5\mathrm{I})6s\ ^6\mathrm{I}_{15/2}$	M1	-	-	0.0008
		3801.917	$4f^4(^5\mathrm{I})6s\ ^6\mathrm{I}_{15/2}$	M1	0.0012	0.0011	0.0009
		4512.481	$4f^4(^5\mathrm{I})6s\ ^4\mathrm{I}_{13/2}$	M1	0.1106	0.1094	0.1084
		5085.619	$4f^4(^5\mathrm{I})6s\ ^6\mathrm{I}_{17/2}$	M1	0.0021	0.0019	0.0015
				$\tau =$	**8.8 s**	**8.8 s**	**9.0 s**
6005.271	$4f^4(^5\mathrm{I})5d\ ^6\mathrm{K}_{9/2}$	0.000	$4f^4(^5\mathrm{I})6s\ ^6\mathrm{I}_{7/2}$	E2	0.0247	0.0254	0.0231
		513.322	$4f^4(^5\mathrm{I})6s\ ^6\mathrm{I}_{9/2}$	E2	0.0032	0.0036	0.0028
		4437.558	$4f^4(^5\mathrm{I})5d\ ^6\mathrm{L}_{11/2}$	M1+E2	0.0012	0.0011	0.0010
				$\tau =$	**34.2 s**	**33.2 s**	**37.0 s**
6637.411	$4f^4(^5\mathrm{I})5d\ ^6\mathrm{L}_{15/2}$	1470.097	$4f^4(^5\mathrm{I})6s\ ^6\mathrm{I}_{11/2}$	E2	0.0109	0.0109	0.0101
		5487.657	$4f^4(^5\mathrm{I})5d\ ^6\mathrm{L}_{13/2}$	M1	0.1669	0.1663	0.1672
				$\tau =$	**5.6 s**	**5.6 s**	**6.0 s**
6931.800	$4f^4(^5\mathrm{I})5d\ ^6\mathrm{K}_{11/2}$	0.000	$4f^4(^5\mathrm{I})6s\ ^6\mathrm{I}_{7/2}$	E2	0.0055	0.0057	0.0055
		513.322	$4f^4(^5\mathrm{I})6s\ ^6\mathrm{I}_{9/2}$	E2	0.0221	0.0225	0.0238
		1470.097	$4f^4(^5\mathrm{I})6s\ ^6\mathrm{I}_{11/2}$	E2	0.0036	0.0041	0.0032
		1650.199	$4f^4(^5\mathrm{I})6s\ ^4\mathrm{I}_{9/2}$	E2	0.0029	0.0027	0.0014
		4437.558	$4f^4(^5\mathrm{I})5d\ ^6\mathrm{L}_{11/2}$	M1	0.0022	0.0021	0.0018
		6005.271	$4f^4(^5\mathrm{I})5d\ ^6\mathrm{K}_{9/2}$	M1	0.0640	0.0637	0.0641
				$\tau =$	**9.9 s**	**9.9 s**	**10.0 s**
7524.740	$4f^4(^5\mathrm{I})5d\ ^6\mathrm{I}_{7/2}$	0.000	$4f^4(^5\mathrm{I})6s\ ^6\mathrm{I}_{7/2}$	E2	0.0637	0.0620	0.0667
		513.322	$4f^4(^5\mathrm{I})6s\ ^6\mathrm{I}_{9/2}$	M1+E2	0.0196	0.0217	0.0146
		6005.271	$4f^4(^5\mathrm{I})5d\ ^6\mathrm{K}_{9/2}$	M1	0.0018	0.0013	0.0015
				$\tau =$	**11.7 s**	**11.7 s**	**12.0 s**
7868.896	$4f^4(^5\mathrm{I})5d\ ^6\mathrm{L}_{17/2}$	2585.453	$4f^4(^5\mathrm{I})6s\ ^6\mathrm{I}_{13/2}$	E2	0.0137	0.0135	0.0124
		6637.411	$4f^4(^5\mathrm{I})5d\ ^6\mathrm{L}_{15/2}$	M1	0.2061	0.2056	0.2055
				$\tau =$	**4.5 s**	**4.6 s**	**4.6 s**

Table 1. *Continued.*

Upper level		Lower level		Type	A_{ki}(s^{-1})		
Energy[a] (cm^{-1})	Designation	Energy[a] (cm^{-1})	Designation		HFR(A)[b]	HFR(B)[c]	GRASP[d]
7950.070	$4f^4(^5\mathrm{I})5d\ ^6\mathrm{K}_{13/2}$	513.322	$4f^4(^5\mathrm{I})6s\ ^6\mathrm{I}_{9/2}$	E2	0.0092	0.0097	0.0094
		1470.097	$4f^4(^5\mathrm{I})6s\ ^6\mathrm{I}_{11/2}$	E2	0.0259	0.0264	0.0256
		2585.453	$4f^4(^5\mathrm{I})6s\ ^6\mathrm{I}_{13/2}$	E2	0.0029	0.0034	0.0027
		5487.657	$4f^4(^5\mathrm{I})5d\ ^6\mathrm{L}_{13/2}$	M1	0.0026	0.0023	0.0022
		6931.800	$4f^4(^5\mathrm{I})5d\ ^6\mathrm{K}_{11/2}$	M1	0.1150	0.1143	0.1152
				$\tau =$	**6.3 s**	**6.3 s**	**6.4 s**
8420.321	$4f^4(^5\mathrm{I})5d\ ^6\mathrm{I}_{9/2}$	0.000	$4f^4(^5\mathrm{I})6s\ ^6\mathrm{I}_{7/2}$	E2	0.0235	0.0243	0.0249
		513.322	$4f^4(^5\mathrm{I})6s\ ^6\mathrm{I}_{9/2}$	E2	0.0484	0.0473	0.0573
		1470.097	$4f^4(^5\mathrm{I})6s\ ^6\mathrm{I}_{11/2}$	E2	0.0175	0.0197	0.0146
		1650.199	$4f^4(^5\mathrm{I})6s\ ^4\mathrm{I}_{9/2}$	M1+E2	0.0084	0.0079	0.0042
		6005.271	$4f^4(^5\mathrm{I})5d\ ^6\mathrm{K}_{9/2}$	M1	0.0034	0.0027	0.0028
		7524.740	$4f^4(^5\mathrm{I})5d\ ^6\mathrm{I}_{7/2}$	M1	0.0568	0.0561	0.0585
				$\tau =$	**6.3 s**	**6.3 s**	**6.1 s**
8716.462	$4f^4(^5\mathrm{I})5d\ ^6\mathrm{G}_{3/2}$	0.000	$4f^4(^5\mathrm{I})6s\ ^6\mathrm{I}_{7/2}$	E2	0.1960	0.2000	0.1884
				$\tau =$	**5.1 s**	**5.0 s**	**5.3 s**
8796.378	$4f^4(^5\mathrm{I})5d\ ^6\mathrm{G}_{5/2}$	0.000	$4f^4(^5\mathrm{I})6s\ ^6\mathrm{I}_{7/2}$	E2	0.0182	0.0180	0.0502
		513.322	$4f^4(^5\mathrm{I})6s\ ^6\mathrm{I}_{9/2}$	E2	0.1380	0.1222	0.1071
				$\tau =$	**6.4 s**	**7.1 s**	**6.3 s**
9042.743	$4f^4(^5\mathrm{I})5d\ ^6\mathrm{K}_{15/2}$	1470.097	$4f^4(^5\mathrm{I})6s\ ^6\mathrm{I}_{11/2}$	E2	0.0112	0.0120	0.0107
		2585.453	$4f^4(^5\mathrm{I})6s\ ^6\mathrm{I}_{13/2}$	E2	0.0301	0.0299	0.0279
		3801.917	$4f^4(^5\mathrm{I})6s\ ^6\mathrm{I}_{15/2}$	E2	0.0019	0.0022	0.0018
		6637.411	$4f^4(^5\mathrm{I})5d\ ^6\mathrm{L}_{15/2}$	M1	0.0022	0.0018	0.0017
		7950.070	$4f^4(^5\mathrm{I})5d\ ^6\mathrm{K}_{13/2}$	M1	0.1394	0.1394	0.1402
				$\tau =$	**5.4 s**	**5.4 s**	**5.5 s**
9166.209	$4f^4(^5\mathrm{I})5d\ ^6\mathrm{L}_{19/2}$	3801.917	$4f^4(^5\mathrm{I})6s\ ^6\mathrm{I}_{15/2}$	E2	0.0163	0.0161	0.0143
		7868.896	$4f^4(^5\mathrm{I})5d\ ^6\mathrm{L}_{17/2}$	M1	0.1935	0.1930	0.1935
				$\tau =$	**4.8 s**	**4.8 s**	**4.8 s**
9198.395	$4f^4(^5\mathrm{I})5d\ ^6\mathrm{G}_{7/2}$	0.000	$4f^4(^5\mathrm{I})6s\ ^6\mathrm{I}_{7/2}$	E2	0.0333	0.0702	0.0190
		513.322	$4f^4(^5\mathrm{I})6s\ ^6\mathrm{I}_{9/2}$	E2	0.0801	0.0931	0.0723
		1470.097	$4f^4(^5\mathrm{I})6s\ ^6\mathrm{I}_{11/2}$	E2	0.0447	0.0007	0.0519
		1650.199	$4f^4(^5\mathrm{I})6s\ ^4\mathrm{I}_{9/2}$	M1+E2	0.0023	0.0179	0.0011
		7524.740	$4f^4(^5\mathrm{I})5d\ ^6\mathrm{I}_{7/2}$	M1	0.0055	0.0084	0.0007
				$\tau =$	**5.9 s**	**5.2 s**	**6.9 s**
9357.906	$4f^4(^5\mathrm{I})5d\ ^6\mathrm{I}_{11/2}$	0.000	$4f^4(^5\mathrm{I})6s\ ^6\mathrm{I}_{7/2}$	E2	0.0021	0.0023	0.0020
		513.322	$4f^4(^5\mathrm{I})6s\ ^6\mathrm{I}_{9/2}$	E2	0.0352	0.0377	0.0366
		1470.097	$4f^4(^5\mathrm{I})6s\ ^6\mathrm{I}_{11/2}$	E2	0.0578	0.0564	0.0596
		2585.453	$4f^4(^5\mathrm{I})6s\ ^6\mathrm{I}_{13/2}$	E2	0.0117	0.0132	0.0119
		3066.750	$4f^4(^5\mathrm{I})6s\ ^4\mathrm{I}_{11/2}$	E2	0.0034	0.0032	0.0019
		6931.800	$4f^4(^5\mathrm{I})5d\ ^6\mathrm{K}_{11/2}$	M1	0.0040	0.0027	0.0036
		8420.321	$4f^4(^5\mathrm{I})5d\ ^6\mathrm{I}_{9/2}$	M1	0.0867	0.0858	0.0886
				$\tau =$	**4.9 s**	**4.9 s**	**5.2 s**
9674.844	$4f^4(^5\mathrm{I})5d\ ^6\mathrm{H}_{5/2}$	0.000	$4f^4(^5\mathrm{I})6s\ ^6\mathrm{I}_{7/2}$	E2	0.2800	0.2900	0.2468
		513.322	$4f^4(^5\mathrm{I})6s\ ^6\mathrm{I}_{9/2}$	E2	0.0223	0.0468	0.0697
		1650.199	$4f^4(^5\mathrm{I})6s\ ^4\mathrm{I}_{9/2}$	E2	0.0096	0.0008	0.0159
		8716.462	$4f^4(^5\mathrm{I})5d\ ^6\mathrm{G}_{3/2}$	M1	0.0087	0.0482	0.0004
		8796.378	$4f^4(^5\mathrm{I})5d\ ^6\mathrm{G}_{5/2}$	M1	0.0021	0.0081	-
				$\tau =$	**3.1 s**	**2.5 s**	**3.0 s**
9877.173	$4f^4(^5\mathrm{I})5d\ ?_{9/2}$	0.000	$4f^4(^5\mathrm{I})6s\ ^6\mathrm{I}_{7/2}$	E2	0.0077	0.0149	0.0035
		513.322	$4f^4(^5\mathrm{I})6s\ ^6\mathrm{I}_{9/2}$	M1+E2	0.0614	0.0913	0.0381
		1470.097	$4f^4(^5\mathrm{I})6s\ ^6\mathrm{I}_{11/2}$	E2	0.0777	0.0723	0.0795
		1650.199	$4f^4(^5\mathrm{I})6s\ ^4\mathrm{I}_{9/2}$	M1+E2	0.0013	0.0048	0.0017
		2585.453	$4f^4(^5\mathrm{I})6s\ ^6\mathrm{I}_{13/2}$	E2	0.0184	0.0005	0.0350
		3066.750	$4f^4(^5\mathrm{I})6s\ ^4\mathrm{I}_{11/2}$	E2	0.0017	0.0061	0.0015

Table 1. *Continued.*

Upper level		Lower level		Type	A_{ki}(s^{-1})		
Energy[a] (cm^{-1})	Designation	Energy[a] (cm^{-1})	Designation		HFR(A)[b]	HFR(B)[c]	GRASP[d]
		6005.271	$4f^4(^5\mathrm{I})5d\ ^6\mathrm{K}_{9/2}$	M1	0.0056	0.0139	0.0011
		6931.800	$4f^4(^5\mathrm{I})5d\ ^6\mathrm{K}_{11/2}$	M1	0.0012	0.0026	-
		9198.395	$4f^4(^5\mathrm{I})5d\ ^6\mathrm{G}_{7/2}$	M1	0.0229	0.0195	0.0262
				$\tau =$	**5.0 s**	**4.4 s**	**5.3 s**
9908.650	$4f^4(^5\mathrm{I})5d\ ?_{7/2}$	0.000	$4f^4(^5\mathrm{I})6s\ ^6\mathrm{I}_{7/2}$	E2	0.0584	0.0113	0.0268
		513.322	$4f^4(^5\mathrm{I})6s\ ^6\mathrm{I}_{9/2}$	E2	0.0629	0.0021	0.0264
		1470.097	$4f^4(^5\mathrm{I})6s\ ^6\mathrm{I}_{11/2}$	E2	0.0947	0.1537	0.0990
		1650.199	$4f^4(^5\mathrm{I})6s\ ^4\mathrm{I}_{9/2}$	E2	0.0066	0.0043	0.0931
		7524.740	$4f^4(^5\mathrm{I})5d\ ^6\mathrm{I}_{7/2}$	M1	0.0008	0.0037	0.0001
		8420.321	$4f^4(^5\mathrm{I})5d\ ^6\mathrm{I}_{9/2}$	M1	0.0042	0.0001	0.0037
		8796.378	$4f^4(^5\mathrm{I})5d\ ^6\mathrm{G}_{5/2}$	M1	0.0304	0.1165	0.0159
		9198.395	$4f^4(^5\mathrm{I})5d\ ^6\mathrm{G}_{7/2}$	M1	0.0030	0.0012	0.0032
				$\tau =$	**3.8 s**	**3.6 s**	**3.7 s**
10194.786	$4f^4(^5\mathrm{I})5d\ ^6\mathrm{K}_{17/2}$	2585.453	$4f^4(^5\mathrm{I})6s\ ^6\mathrm{I}_{13/2}$	E2	0.0099	0.0111	0.0092
		3801.917	$4f^4(^5\mathrm{I})6s\ ^6\mathrm{I}_{15/2}$	E2	0.0329	0.0333	0.0308
		9042.743	$4f^4(^5\mathrm{I})5d\ ^6\mathrm{K}_{15/2}$	M1	0.1300	0.1300	0.1308
				$\tau =$	**5.7 s**	**5.7 s**	**5.8 s**
10337.097	$4f^4(^5\mathrm{I})5d\ ^6\mathrm{I}_{13/2}$	513.322	$4f^4(^5\mathrm{I})6s\ ^6\mathrm{I}_{9/2}$	E2	0.0046	0.0047	0.0037
		1470.097	$4f^4(^5\mathrm{I})6s\ ^6\mathrm{I}_{11/2}$	E2	0.0364	0.0401	0.0426
		2585.453	$4f^4(^5\mathrm{I})6s\ ^6\mathrm{I}_{13/2}$	E2	0.0651	0.0641	0.0774
		3801.917	$4f^4(^5\mathrm{I})6s\ ^6\mathrm{I}_{15/2}$	E2	0.0067	0.0076	0.0077
		7950.070	$4f^4(^5\mathrm{I})5d\ ^6\mathrm{K}_{13/2}$	M1	0.0035	0.0022	0.0033
		9357.906	$4f^4(^5\mathrm{I})5d\ ^6\mathrm{I}_{11/2}$	M1	0.0964	0.0971	0.0977
				$\tau =$	**4.6 s**	**4.6 s**	**4.3 s**

[a] The level values are taken from Martin et al. [15]. [b] HFR(A): Relativistic Hartree-Fock calculations including the $4f^45d$ and $4f^46s$ configurations. [c] HFR(B): Relativistic Hartree-Fock calculations including the $4f^45d$, $4f^46s$, $4f^35d6p$, $4f^36s6p$, $4f^25d^26s$,$4f^25d6s^2$ and $4f^25d^3$ configurations. [d] GRASP: see the text.

The AST transition probabilities (A_{ki}, in s^{-1}) as obtained for the two levels considered experimentally (see further) are not reported in Table 1. The values were 0.0025 and 0.0634 s^{-1} for the two M1 transitions emitted from the level at 6931.800 cm^{-1} to the levels at 4437.558 and 6005.271 cm^{-1} and 0.008, 0.0023, 0.0961 s^{-1} for the three transitions depopulating the level at 10337.097 cm^{-1} to those situated at 6931.800, 7950.070 and 9357.906 cm^{-1}. They agree well with the GRASP results.

Some of the even-parity levels considered in the present work are located above odd-parity levels belonging to the $4f^35d^2$ configuration (i.e. those situated at 8009.810 cm^{-1} and 10091.380 cm^{-1}) or to the $4f^35d6s$ configuration (those at 10054.195 and 10091.360 cm^{-1}) and, consequently, electric dipole transitions (E1) could play a role in the radiative decay of high even levels reported in Table 1. In fact, the even levels situated at 9357.906 ($J = 11/2$) and 10337.097 cm^{-1}($J = 13/2$) can give rise to E1 transitions to the odd-level situated at 8009.810 cm^{-1}. For those allowed transitions, it was verified that the decay rates were negligible when compared to the ones calculated for the M1 and E2 channels. Indeed, a simple HFR calculation, including the $4f^46s$, $4f^45d$ and $4f^35d^2$ configurations showed that the corresponding E1 transition probabilities should be of the order of 10^{-6} s^{-1} which is five orders of magnitude smaller than the forbidden transition decay rates. For the levels at 9042.743 and 10194.786 cm^{-1}, it was verified that the far infrared decay transitions play also a negligible role in the present context.

4 Experimental work

Natural radiative lifetimes of metastable states may range from milliseconds up to years. Under ordinary vacuum conditions that can be obtained in the laboratory, the frequency of collisions with neighbouring atoms or molecules is high compared to the radiative decay rates of the forbidden transitions and the levels will primarily be depopulated by collisions. Besides this complication, it is also necessary to store the ions for a time sufficiently long to observe the decay. We have developed a laser probing technique (LPT) [12,36] at the ion storage ring CRYRING [35] at the Manne Siegbahn Laboratory of Stockholm University where the present measurements were performed.

Long lifetimes mean very low decay rate and, consequently, the emission from natural radiative decay will be extremely weak and passive observation would be very difficult. In the LPT, an allowed transition from the

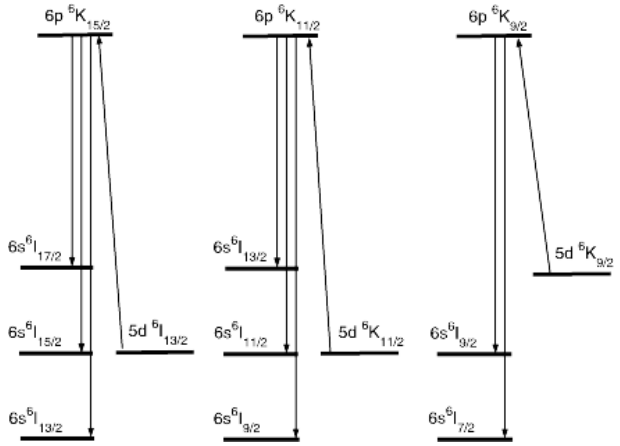

Fig. 1. Schematic level diagram showing the laser transitions and the observed fluorescence used in measurements of lifetimes of three different metastable levels.

metastable level to an upper level is induced by a laser (Fig. 1). The upper level will decay promptly (in nanoseconds) and this fluorescence is proportional to the population of the metastable level. With laser excitation performed in front of a photodetector, the fluorescence can be recorded with very high efficiency. Collinear laser excitation, in addition, also offers high spectral resolution permitting studies of ions with complex spectra as e.g. Fe II [37] and also hyperfine resolved studies [38,39]. The method has so far been used to measure lifetimes up to 28 s [40].

The measurements made at CRYRING have been widely discussed in recent review papers [12,41] and a detailed discussion will not be repeated here. We shall only briefly describe the specificities of the experiment carried out in the case of Nd II.

Singly charged Nd ions were produced in a low-voltage, hot cathode ion source from neodymium chloride and were accelerated by a voltage of 40 kV. The ion beam was mass-separated in a 90° bending magnet, where $^{142}Nd^+$ ions were selected and injected into the storage ring, in which the ions were trapped by twelve dipole magnets and a number of focusing quadrupoles. The stored ion current in the present experiment was a few hundreds of nA. A small fraction of the stored beam consisted of ions in metastable levels that were populated in the ion source. There were severe difficulties in maintaining a stable discharge in the ion source and, consequently, it was hard to keep a stable ion beam in the ring. Also the fraction of metastable level population extracted from the source sometimes fluctuated and caused problems.

The ions were stored at a base pressure less than 10^{-11} torr. For singly charged ions at a beam energy of 40 keV, the primary process responsible for the ion loss is neutralization by collisions with the rest gas. This process limited the lifetime of the stored ion beam to about one minute. The decay was monitored with a BaF_2 scintillator detector and a photomultiplier positioned after one of the dipole magnets monitoring neutralized particles. Ion beam current decay curves were also recorded by a multichannel plate detector for neutralized ions placed after another bending magnet.

In order to determine the radiative lifetime of a metastable level it is necessary to account for other processes, mainly collisional effects, that influence the population of the level. Collisions with the residual gas may both excite, deexcite and neutralize the stored ions. We have developed methods to account for these effects as described in [12,41], for instance. Such effects are usually small but necessary to correct for.

LPT is a sequential method. Only one point on the decay curve can be measured for a specific injection pulse of ions into the storage ring. A new injection is needed for every new point. Therefore it is important to monitor the intensity of each injection pulse. It is also necessary to monitor the metastable fraction and the efficiency of the laser excitation. Such normalization curves are recorded together with the decay curve of the metastable level [12], see Figure 2. In the present case the instabilities seem to have been too severe to handle completely with this method since decay curves for a certain level did not reproduce well even if they had been corrected by the normalization curves. Such problems have not been met before. Afterwards we have tried to make sensible judgments of which data could be trusted. The spread between different measurements were in this case often much larger than the statistical uncertainty of a single curve. Due to these problems we are not confident on the results and the results should in this case more be regarded as a qualitative check of the calculations.

5 Results and discussion

The two sets of HFR results reported in Table 1 indicate however that the present lifetimes are not very sensitive to the configuration sets considered in the models. It is expected also that adding additional configurations would affect more the E2 contributions than the M1 channels. As these E2 channels are not the dominant ones, including additional configuration interaction (prevented in the present work by the computer limits) would probably have a marginal effect on the calculated lifetime values. The effect of higher order contributions (M2, E3, M3, ...) was found to be negligible.

In addition, the agreement between the results obtained by two different independent theoretical methods (HFR and GRASP), this agreement being also confirmed by the M1 transition probabilities calculated using the AST method, is an argument in favour of the present results.

The experimental lifetimes, as deduced in the present work for the two levels $4f^4(^5I)5d\ ^6K_{11/2}$ and $4f^4(^5I)5d\ ^6I_{13/2}$ at 6931.800 and 10337.097 cm^{-1} (see Fig. 3), were 23.0 and 8.4 s but, as stated above, they must be considered only as indicative of the true values. In Figure 4 we show a measurement of the lifetime of the $^6K_{9/2}$ levels that supports the calculated very long lifetime (34 s) of this level.

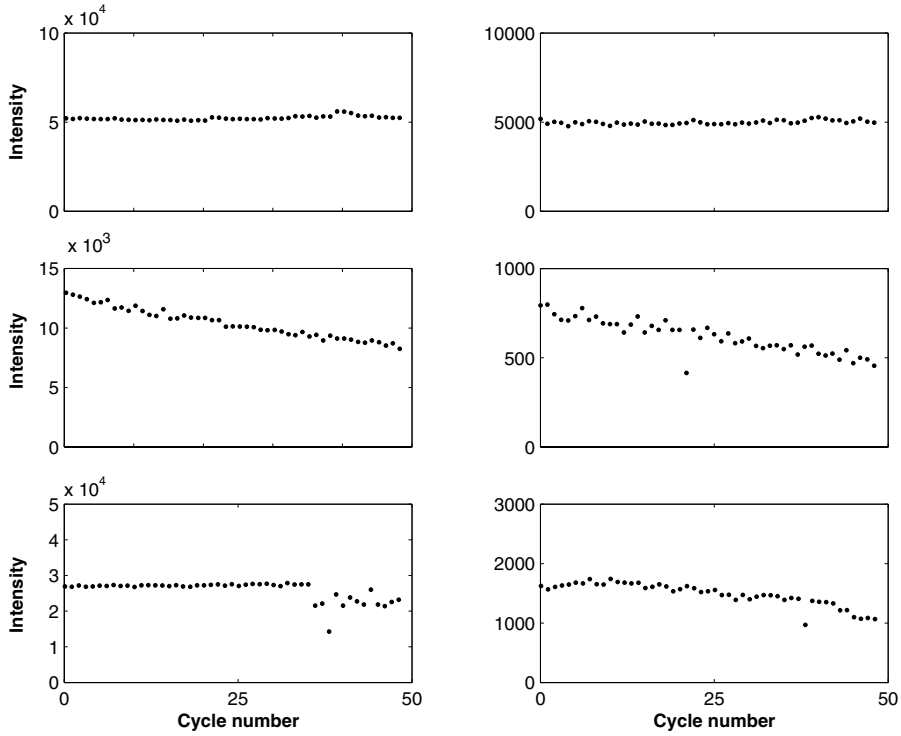

Fig. 2. Different examples of normalization curves obtained in the measurement of a lifetime curve. The left column shows particle normalization curves that reflect the number of stored ions for different ion injections. The right column shows fluorescence normalization for different ion injections. This signal reflects the number of ions in the metastable state. The curves are connected pair wise, i.e. for a constant metastable fraction of injected ions the ratio between the left and the right curve should be constant. The upper curve is an example of a measurement of the $^6I_{13/2}$ recorded at base pressure. Here both particle intensity and metastable fraction are stable during the measurement and normalization gives minor contributions in the analysis. This is a typical situation for our previous experiment utilizing LPT. In the second row, which is another measurement of the same level, both particle and metastable intensities drop strongly during the measurement and the normalization is important. The last row is a measurement of the $^6K_{11/2}$ at base pressure. Here the conditions are unstable and the peculiar situation arises where the two curves do not follow each other, indicating that the conditions in the ion source are not stable enough to keep the metastable fraction constant. In this case normalization is important.

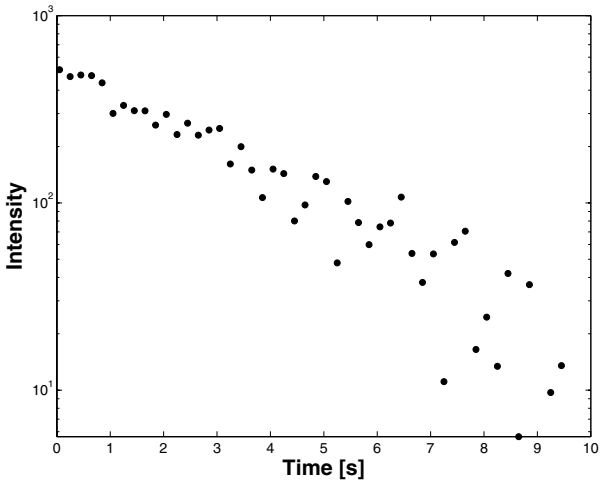

Fig. 3. A lifetime curve obtained in a measurement of the $^6I_{13/2}$ level in Nd II at raised pressure in the ring. The plotted data has been normalized and corrected for repopulation. This is one of the best measurements in Nd II as regards statistics and stability in the measurement conditions.

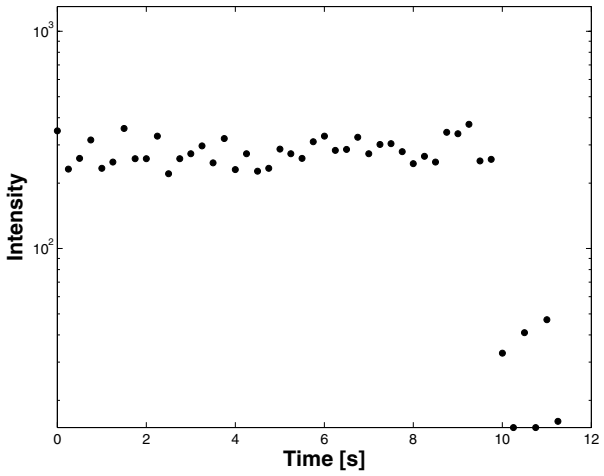

Fig. 4. Raw data of two separate measurements of the $^6K_{9/2}$ level. Due to lack of repopulation measurements no lifetime value could be extracted but the lifetime is obviously consistent with the calculated value of 34 s.

This work was supported by the Swedish Research Council (VR). The work of the whole staff of the CRYRING facility was highly appreciated. E.B. is Research Director of the Belgian National Fund for Scientific Research, P.P. and P.Q. are Research Associates of the same organization. Financial support from the Institut Interuniversitaire des Sciences Nucléaires is also acknowledged.

References

1. S. Adelman, Astrophys. J. Suppl. **26**, 1 (1973)
2. C.R. Cowley, H.M. Crosswhite, P.A.S.P. **90**, 108 (1978)
3. M.A. Smith, Astrophys. J. **189**, 101 (1974)
4. D.L. Lambert, in *Cools Stars with Excesses of Heavy Elements*, edited by M. Jaschek, P.C. Keenan (Reidel, 1985)
5. R.S. Maier, W. Whaling, J. Quant. Spectrosc. Radiat. Transfer **18**, 501 (1977)
6. M. Asplund, N. Grevesse, A.J. Sauval, In *Cosmic Abundances as Records of Stellar Evolution and Nucleosynthesis*, edited by F.N. Bash, T.G. Barnes, ASP Conf. Ser., San Francisco, Vol. XXX (2005)
7. R.C.M. Learner, J. Davies, A.P. Thorne, Mont. Not. Roy. Astron. Soc. **248**, 414 (1991)
8. M. Eriksson, U. Litzén, G.M. Wahlgrén, D.S. Leckrone, Phys. Scripta **65**, 480 (2002)
9. É. Biémont, Phys. Scripta T**119**, 55 (2005)
10. É. Biémont, P. Quinet, Phys. Scripta T**105**, 38 (2003)
11. Database DREAM on the site `http://www.umh.ac.be/~astro/dream.shtml`
12. S. Mannervik, Phys. Scripta T**105**, 67 (2003)
13. A. Derkatch, L. Ilyinsky, S. Mannervik, L.-O. Norlin, D. Rostohar, P. Royen, P. Schef, É. Biémont, Phys. Rev. A **65**, 062508 (2002)
14. D. Rostohar, A. Derkatch, H. Hartman, S. Mannervik, L.-O. Norlin, P. Royen, A. Schmitt, X. Tordoir, Phys. Scripta **64**, 237 (2001)
15. W.C. Martin, R. Zalubas, L. Hagan, *Atomic Energy Levels, The Rare Earth Elements*, NSRDS-NBS **60** (1978) and NIST database on line
16. J. Blaise, J.-F. Wyart, M.T. Djerad, Z.B. Ahmed, Phys. Scripta **29**, 119 (1984)
17. C.H. Corliss, W.R. Bozman, Nat. Bur. Stand. (U.S.), Monogr. **53**, 256 (1962)
18. T. Andersen, O. Poulsen, P.S. Ramanujam, A.P. Petkov, Sol. Phys. **44**, 257 (1975)
19. L. Ward, O. Vogel, A. Ahnesjoe, A. Arnesen, R. Hallin, L. McIntyre, C. Nordling, Phys. Scripta **29**, 551 (1984)
20. L. Ward, O. Vogel, A. Arnesen, R. Hallin, A. Wännström, Phys. Scripta **31**, 161 (1985)
21. J. Reader, C.H. Corliss, W.L. Wiese, G.A. Martin, *Wavelengths and Transition Probabilities for Atoms and Atomic Ions*, NSRDS-NBS 68 (1980)
22. K.B. Blagoev, V.A. Komarovskii, At. Data Nucl. Data Tables **56**, 1 (1994)
23. V.N. Gorshkov, V.A. Komarovskii, A.L. Osherovich, N.P. Penkin, Astrophysics (USSR) **17**, 437 (1982)
24. C.M. Pinciuc, R.C. Rivest, M.R. Izawa, R.A. Holt, S.D. Rosner, T.J. Scholl, Can. J. Phys. **79**, 1159 (2001)
25. F. Lu, S. Wu, W. Shi, P. Shi, J. Yang, L. Song, J. Tang, F. Yang, Chin. Phys. Lett. **6**, 161 (1989)
26. W. Shi, F. Lu, S. Wu, P. Shi, J. Yang, L. Song, J. Tang, F. Yang, Phys. Rev. A **43**, 1451 (1991)
27. T.J. Scholl, R.A. Holt, D. Masterman, R.C. Rivest, S.D. Rosner, A. Sharikova, Can. J. Phys. **80**, 713 (2002)
28. H.L. Xu, S. Svanberg, R.D. Cowan, P.-H. Lefèbvre, P. Quinet, É. Biémont, Mont. Not. Roy. Astron. Soc. **346**, 433 (2003)
29. R.D. Cowan, *The Theory of Atomic Structure and Spectra* (Univ. California Press, Berkeley, Calif., USA, 1981)
30. F. Parpia, C. Froese Fischer, I.P. Grant, Comput. Phys. Commun. **94**, 249 (1996)
31. N.R. Badnell, J. Phys. B **19**, 3827 (1986)
32. N.R. Badnell, J. Phys. B **30**, 1 (1997)
33. W. Eissner, M. Jones, H. Nussbaumer, Comput. Phys. Commun. **8**, 270 (1974)
34. W. Eissner, H. Nussbaumer, J. Phys. B **2**, 1028 (1969)
35. K. Abrahamsson et al., Nucl. Instr. Meth. Phys. Res. B **79**, 268 (1993)
36. J. Lidberg, A. Al-Khalili, L.O. Norlin, P. Royen, X. Tordoir, S. Mannervik, Nucl Instr. Meth. Phys. Res. B **152**, 157 (1999)
37. D. Rostohar, A. Derkatch, H. Hartman, S. Johansson, H. Lundberg, S. Mannervik, L.-O. Norlin, P. Royen, A, Schmitt, Phys. Rev. Lett. **86**, 1466 (2001)
38. S. Mannervik, L. Broström, J. Lidberg, L.-O. Norlin, P. Royen, Phys. Rev. Lett. **76**, 3675 (1996)
39. P. Schef, P. Lundin, É. Biémont, A. Källberg, L.-O. Norlin, P. Palmeri, P. Royen, A. Simonsson, S. Mannervik, Phys. Rev. A **72**, 020501 (2005)
40. H. Hartman, D. Rostohar, A. Derkatch, P. Lundin, P. Schef, S. Johansson, H. Lundberg, S. Mannervik, L.-O. Norlin, P. Royen, J. Phys. B: At. Mol. Opt. Phys. **36**, L197 (2003)
41. S. Mannervik, A. Ellmann, P. Lundin, L.-O. Norlin, D. Rostohar, P. Royen, P. Schef, Phys. Scripta T**119**, 49 (2005)